Automated method for tracing leading and trailing processes of migrating neurons in confocal image sequences

Ryan A. Kerekes[a], Shaun S. Gleason[a], Niraj Trivedi[b], and David J. Solecki[b]

[a]Oak Ridge National Laboratory, Oak Ridge, TN, USA;
[b]St. Jude Children's Research Hospital, Memphis, TN, USA

ABSTRACT

Segmentation, tracking, and tracing of neurons in video imagery are important steps in many neuronal migration studies and can be inaccurate and time-consuming when performed manually. In this paper, we present an automated method for tracing the leading and trailing processes of migrating neurons in time-lapse image stacks acquired with a confocal fluorescence microscope. In our approach, we first locate and track the soma of the cell of interest by smoothing each frame and tracking the local maxima through the sequence. We then trace the leading process in each frame by starting at the center of the soma and stepping repeatedly in the most likely direction of the leading process. This direction is found at each step by examining second derivatives of fluorescent intensity along curves of constant radius around the current point. Tracing terminates after a fixed number of steps or when fluorescent intensity drops below a fixed threshold. We evolve the resulting trace to form an improved trace that more closely follows the approximate centerline of the leading process. We apply a similar algorithm to the trailing process of the cell by starting the trace in the opposite direction. We demonstrate our algorithm on two time-lapse confocal video sequences of migrating cerebellar granule neurons (CGNs). We show that the automated traces closely approximate ground truth traces to within 1 or 2 pixels on average. Additionally, we compute line intensity profiles of fluorescence along the automated traces and quantitatively demonstrate their similarity to manually generated profiles in terms of fluorescence peak locations.

Keywords: neuron migration, image segmentation, tracing

1. INTRODUCTION

Recent advances in confocal microscopy have allowed neurobiologists to capture the progression of neuronal migration in unprecedented detail. Time-lapse imagery of migrating cells expressing one or more fluorescent proteins can reveal complex mechanical phenomena in action by highlighting the movement of subcellular structures and associated proteins as well as the overall motion of the cell. A problem of recent interest in neuronal migration studies is the analysis of various protein concentrations within the soma body and along the leading and trailing processes of the migrating cell, which are protrusions of the cellular material along the path of migration.[1] Imaging these proteins over periods of several minutes has revealed a correlation between the movement of certain proteins along the leading process and the movement of the soma.

Performing quantitative analysis on this type of imagery, however, can be a daunting task, especially when many video frames need to be processed. For example, quantifying protein concentrations along the extent of the cell requires first "tracing" the processes of the cell, i.e., constructing a curve that follows the centerline; fluorescent intensity can then be measured along this trace. Manual tracing of cells in video amounts to clicking a succession of points along the leading and trailing processes in every frame, which can be inconsistent, inaccurate, and highly time-consuming.

We introduce a method for automatically tracing the leading and trailing processes of migrating neurons in time-lapse sequences of confocal fluorescence microscope images. The resulting trace follows the approximate centerline of the leading and trailing processes. This trace, which can be computed in only one or two seconds

Further author information: (Send correspondence to R.A.K.)
R.A.K.: E-mail: kerekesra@ornl.gov, Telephone: 1 865 576 7847
S.S.G.: E-mail: gleasonss@ornl.gov, Telephone: 1 865 574 8521

per frame on a single Intel Core2 processor running MATLAB, can be used in place of a manual trace to quantify neuron shape and protein concentration along the length of the migrating cell. By applying our algorithm to 50 frames from two migrating neuron video sequences and quantitatively comparing the resulting traces to ground truth, we demonstrate that our method is robust to irregularities along the process such as small protrusions and interference from other neurons in the culture.

Many algorithms have been proposed in the literature for soma detection and neurite tracing in 2-D and 3-D confocal images;[2–5] however, most of these algorithms are designed for single images of fully developed neurons, whose structure and appearance tend to be more constant within a given dataset than that of developing, migrating neurons. In particular, the length and width of the leading process can vary drastically, with length ranging from near zero to hundreds of pixels in the same sequence. We highlight two main novelties of our tracing algorithm: (1) using video in the tracing process, including the use of soma motion to aid in locating the leading and trailing processes and the use of curve evolution to locate the trailing process in subsequent frames; and (2) using 1-D local maxima along concentric arcs to locate the neuronal process, which provides invariance to the width of the process. We believe this work represents a new capability in quantitative neuronal migration image analysis.

2. TECHNICAL APPROACH

Our approach to tracing the leading and trailing processes of a cell can be divided into three stages: (1) locating and tracking the soma; (2) tracing the leading process; and (3) tracing the trailing process. We use information from the soma tracking to guide the subsequent tracing procedures. We describe these stages in more detail below.

2.1 Tracking the soma

Each frame is composed of two channels, one of which uses red fluorescent protein (RFP) to label cytoplasm and the other of which uses green fluorescent protein (GFP) to label actin. In order to track somas, we use the red channel only, where the somas tend to appear more brightly than in the green channel. We first smooth each frame of the video sequence using a 2-D Gaussian filter of radius approximately equal to that of a typical soma. This pre-filtering step accentuates the somas in the scene, causing them to appear as smooth bright blobs. We then locate the local intensity maxima in each frame, the brightest of which should correspond to the approximate centers of the somas. These local maxima are the soma "detections". The user may select one or more local maxima in the first frame that correspond to the somas of interest; alternatively, the brightest N local maxima may be considered with no input required from the user. This concept is illustrated in Fig. 1.

Once the local maxima of interest have been identified in the first frame, we track each of these points throughout the video sequence using a simple nearest neighbor tracking algorithm. Specifically, for a given point in frame 1, we find the nearest local maximum in frame 2 and associate these two points to one another in order to form a track. This procedure continues for every pair of frames i and $i+1$ until the end of sequence is reached. Each resulting track provides an estimate of the center of the corresponding soma in every frame. Such a simple tracking approach is sufficient for this application since the somas tend to maintain a reasonable separation distance. In addition, because of the heavy smoothing in the pre-processing stage, false detections are seldom located closely enough to the true soma detections to cause confusion. After tracking is complete, we compute the average direction of motion of the cell as the direction of the vector extending from the first point of the track to the last point.

2.2 Tracing the leading process

For each soma tracked in the video sequence, we compute the trace of the leading process in each frame by starting at the center of the soma (as given by the soma track) and iteratively stepping outward along the leading process by a predefined distance (e.g., 2 pixels). At each point, we compute the optimal stepping direction to the next point, i.e., the direction most likely to follow the centerline of the leading process as it extends outward from the soma. Once the end of the leading process is reached, the contour defined by the resulting sequence of points is the trace. This concept is illustrated in Fig. 2.

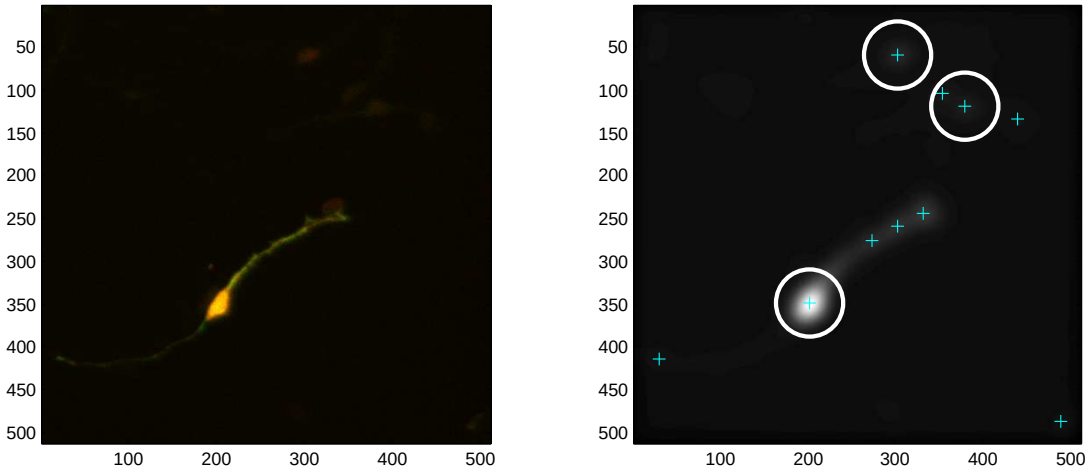

Figure 1. One frame of soma tracking. The original two-channel (red and green) image is shown on the left. The Gaussian-blurred version of the red channel is shown on the left; local maxima are marked with a "+", and the somas of interest are marked with a large circle.

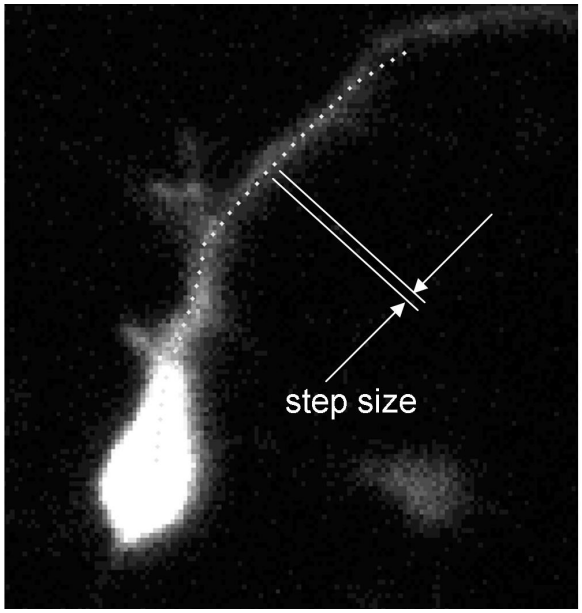

Figure 2. Sequence of trace points for a single frame of a migrating neuron sequence. The step size is a fixed parameter of the algorithm.

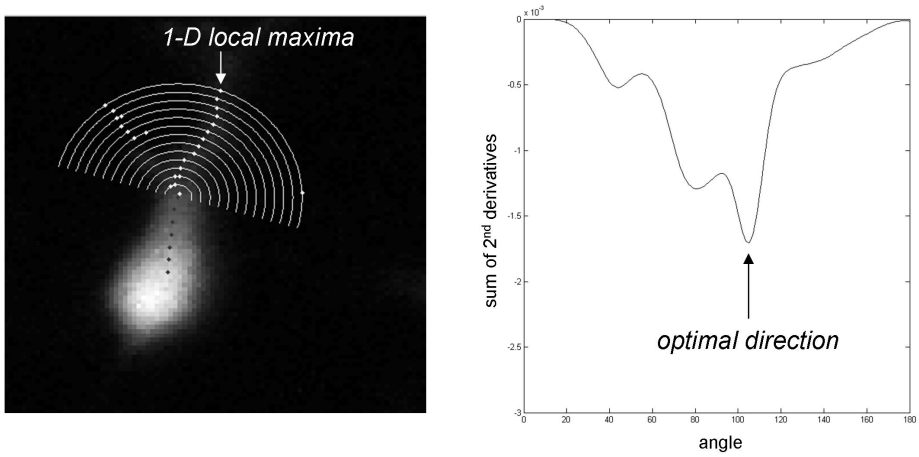

(a) (b)

Figure 3. (a) Arcs centered about the current step point. One-dimensional local maxima along each arc are shown as bright dots. (b) Sum of second derivatives at each local maximum for each one-degree angular bin within the 180-degree range. Because second derivatives at local maxima are always negative, the optimal stepping angle is the one with the minimum sum.

2.2.1 Stepping along the process

At each step, we consider a 180-degree range of potential stepping directions. During the first step, we center this search range about the average motion direction of the soma, which provides a reasonable indication of the direction of the leading process. At subsequent steps, we center the search range about the previous step direction; this effectively prevents the trace from turning more than 90 degrees at each step (which might enable the trace to double back on itself).

Once the range of possible stepping angles is determined, we construct arcs over this angular range at increasing radii centered around the current point. For each arc, we interpolate the image intensity along the arc to construct a one-dimensional intensity function. We locate all local maxima along this profile (illustrated in Fig. 3(a)) and record the direction. We then compute the one-dimensional second derivative at each local maximum along the arc; a highly negative second derivative serves as a potential indicator of the centerline of some curvilinear structure orthogonal to the arc. We partition the 180-degree range of possible stepping directions into 180 bins of width one degree and, for each bin, sum the second derivatives of all the local maxima falling into that bin. This "response function" over the range of angles is smoothed using a Gaussian to remove noise artifacts. We choose as the winner the bin with the most negative response (illustrated in Fig. 3(b)), and this bin becomes the optimal stepping direction from the current point. This procedure is repeated for each subsequent step and terminates after a predefined number of steps. We set the number of steps to be longer than the longest expected process length in order to ensure that the entire process is traced. After post-processing the trace (as described below), we crop the trace at the point where the intensity of the underlying image falls below a predefined threshold, signifying that the boundary of the cellular material has been reached.

2.2.2 Contour evolution

When protrusions, or short branches, are present in the leading process, the process may appear to "fork" at certain points along the path. In this case, the maximum arc radius must be such that the algorithm looks far enough ahead to avoid following the protrusion rather than the true process. An example of this phenomenon is shown in Fig. 4. One side effect of looking ahead, however, is that the algorithm will tend to round off any sharp corners in the path. In order to solve this problem, we adjust the resulting trace after the tracing process is complete. Specifically, we evolve the curve to lie closer to the true centerline by applying a gradient descent-type algorithm to each point along the trace, allowing the point to move in a direction normal to the curve at that point. The amount of adjustment δ_i at each contour point $\mathbf{x}_i$ is determined by maximizing the following objective

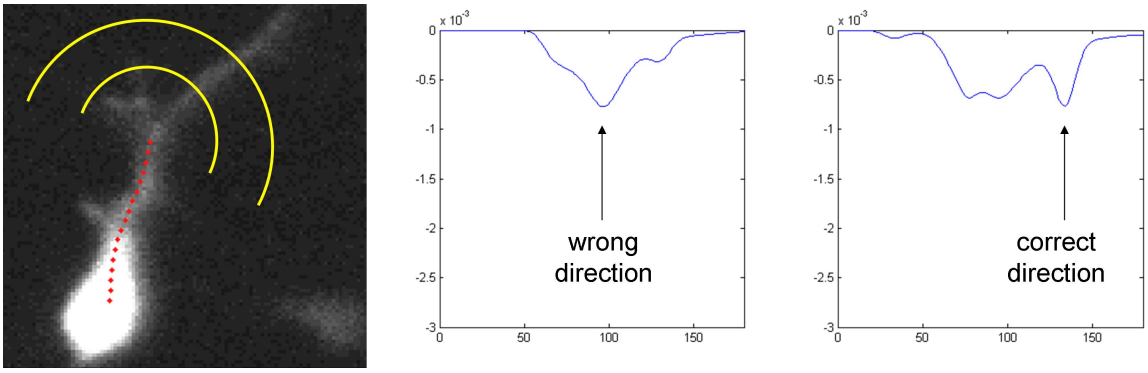

(a) (b) (c)

Figure 4. (a) Arcs of two different radii (20 pixels and 35 pixels) centered about the current step point. (b) Sum of second derivatives for the 20-pixel-radius arc. (c) Sum of second derivatives for the 35-pixel-radius arc. In this case, the stepping algorithm must look more than 20 pixels out in order to avoid taking a wrong turn.

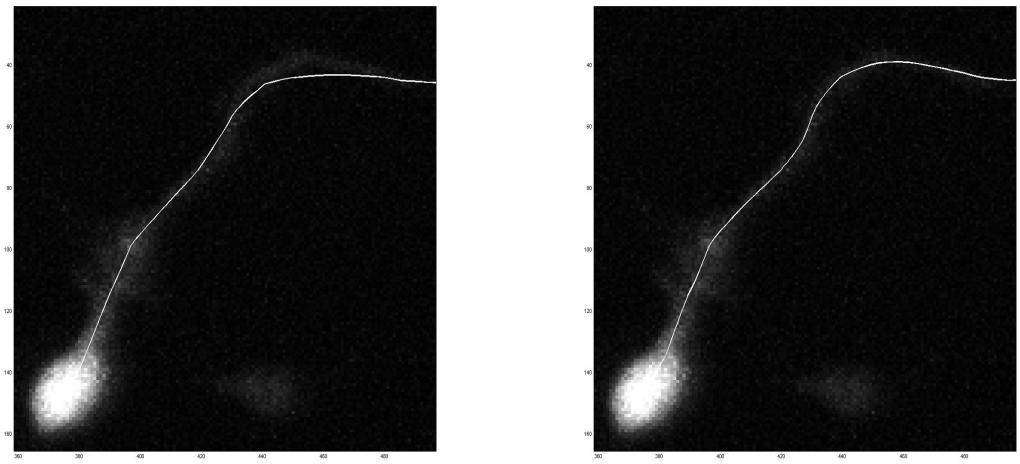

(a) (b)

Figure 5. Example of contour evolution: (a) trace before evolution; (b) trace after evolution. The corner-cutting phenomenon is evident in the pre-evolution contour.

function $J(\delta_i)$:

$$J(\delta_i) = I(\mathbf{x}_i + \delta_i \cdot \mathbf{n}_i) - \alpha \cdot \delta_i \tag{1}$$

where $I(\mathbf{x}_i)$ and $\mathbf{n}_i$ are the image intensity and normal to the curve at $\mathbf{x}_i$, respectively. The second term on the right-hand side of Eq. 1 amounts to a contour deformation penalty, and α is a weighting term for which we used a value of 200. We iteratively loop through the entire set of points $\{\mathbf{x}_i\}$, adjusting one point at a time, until the total adjustment of the curve becomes smaller than a predefined threshold, and we take the adjusted curve as our resulting trace.

2.3 Tracing the trailing process

Once the leading process has been traced, we proceed to trace the trailing process. This portion of the cell is typically dimmer and more difficult to trace than the leading process. In the first frame of the sequence, we apply the same tracing algorithm as above, stepping until termination and then evolving the curve, but using a starting direction opposite that of the leading process, since they typically extend in opposite directions from the soma. In subsequent frames, however, we avoid the stepping process altogether and instead simply evolve

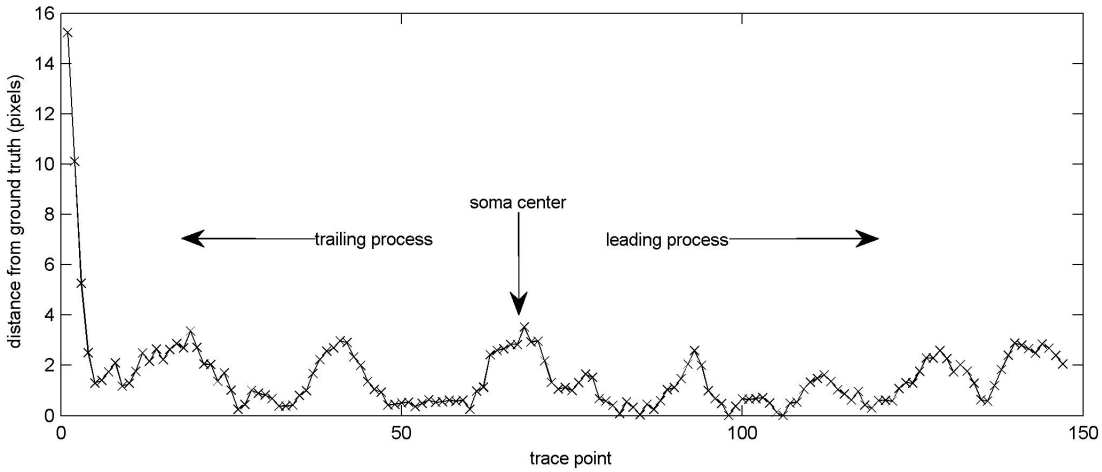

Figure 6. Plot of error (in pixels) along the length of an automated tracing result. The greatest error is observed at the end of the trailing process, where, in this particular example, the cellular material widens and the centerline becomes less well-defined.

the trace computed from the previous frame to match the trailing process in the current frame. This scheme helps to avoid tracing errors resulting from patches of low fluorescence in some regions of the trailing process.

3. RESULTS

We applied our tracing algorithm to two neuron migration sequences. Each sequence contains several migrating neurons in the field of view. For each frame in these two videos, a manual trace was constructed for the brightest neuron using a commercially available software package called Slidebook^{TM}, which provides the capability to draw image masks for marking and analyzing specific regions of an image or volume. Each frame is a two-channel 3-D volume, where green fluorescent protein (GFP) was used to label actin, or cytoskeletal material, and red fluorescent protein (RFP) was used to label cytoplasm. Prior to processing, each two-channel volume was compressed into a 2-D color image by computing the max along the z-dimension at each (x, y) location in each channel. We used the RFP channel for all tracing computations due to greater uniformity in labeling the cellular material.

First, we compare our automated traces to manually generated ground truth traces. We performed a quantitative comparison by computing the distance (in pixels) from each point on the automated trace to its nearest point on the manual trace and averaging over all the points in the automated trace. Tracing results from three sample frames of sequence 1 are shown in Table 1 below. For these frames, average errors are on the order of 2 pixels. The greatest errors typically occur at the far end of the leading and trailing processes, where a widening of the process is frequently observed. This widening causes the centerline of the process to be less well-defined, and thus we expect more variability in these regions.

Fig. 6 shows the error along the automated trace for the first frame of sequence 1. We observe the greatest error at the tip of the trailing process in this trace. Fig. 7 shows the average and maximum error along the automated trace for each frame of the two video sequences; in addition, the portion of the trace in the frame that contributed to the largest maximum trace error in each sequence is shown. While the maximum errors appear large in these graphs, these errors only tend to occur at the end of the leading and trailing process; thus, the average error is a better metric for assessing overall performance. Table 2 summarizes these error metrics for the two sequences. The average errors (on the order of two pixels) are significantly smaller than the typical width of the neuronal processes (on the order of 10 pixels), suggesting good performance from the automated tracing algorithm.

Second, in Fig. 8 we show line intensity profiles of GFP and RFP fluorescence computed along the automated and manual traces for the first frame of the video sequence. We observe that actin peaks are detected in approximately the same locations by both methods. The intensity values of the automated profiles tend to be

Table 1. Comparison of tracing results for three frames (1, 5, and 10) of sequence 1.

Manual trace	Automated trace	Avg. error (pixels)
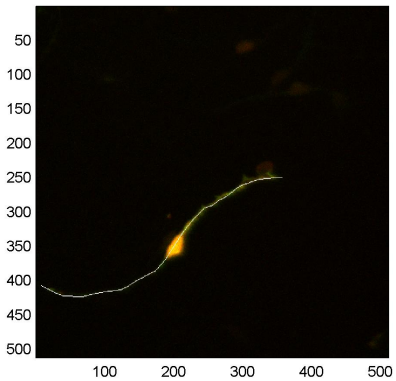	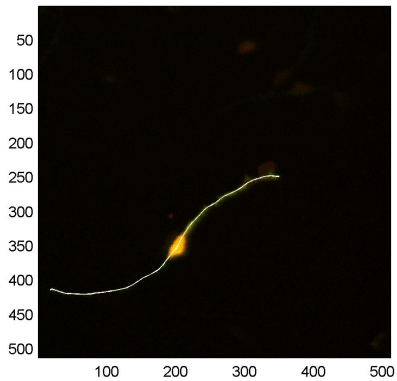	1.31
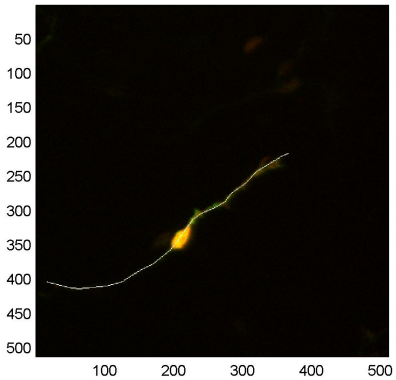	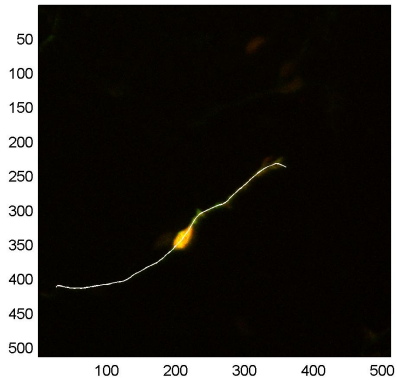	1.53
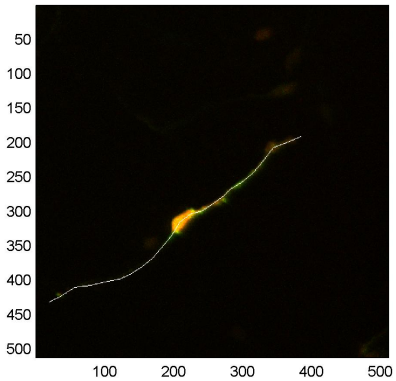	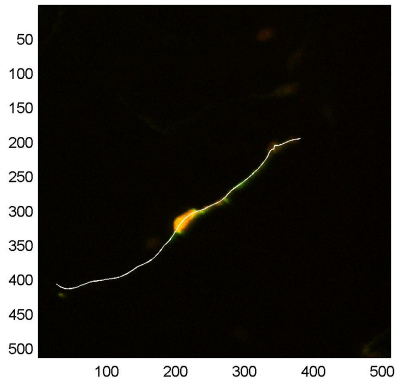	2.27

Table 2. Comparison of tracing results for all frames of sequences 1 and 2.

Sequence	Number of frames	Avg. error (pixels)	Std. dev. (pixels)
1	32	1.87	0.36
2	18	2.05	0.49

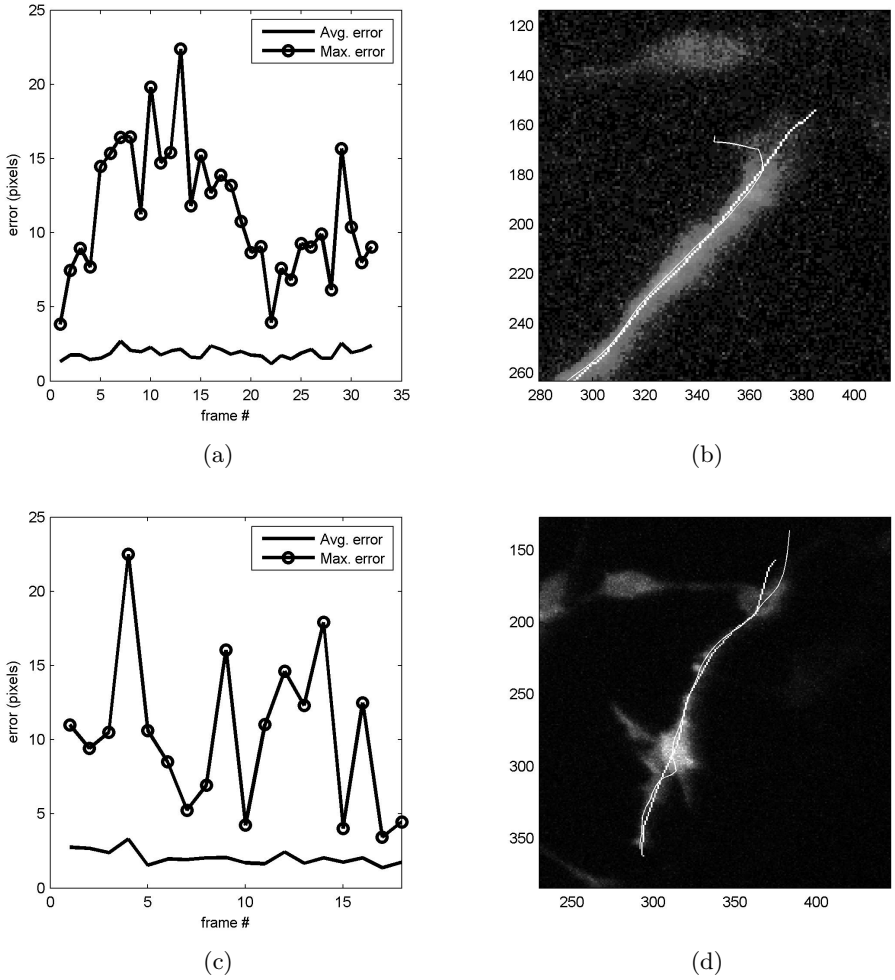

Figure 7. Plots of average and maximum error over each trace for all frames of (a) sequence 1 and (c) sequence 2. Also, magnification of trace results at the tip of the leading process for (b) frame 13 of sequence 1 and (d) frame 4 of sequence 2, where the greatest errors occurred. The thinner line is the automated trace. The automated traces only deviated severely at the end of the leading and trailing processes, resulting in large maximum errors but small average errors.

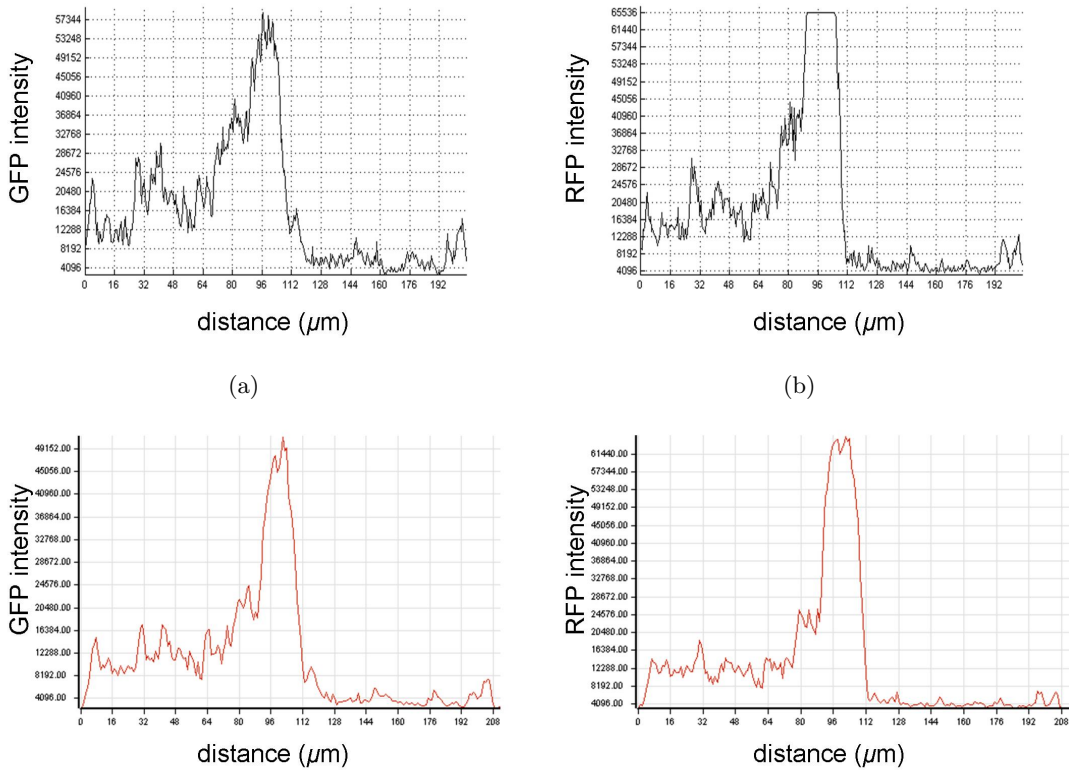

(a) (b)

(c) (d)

Figure 8. Comparison of fluorescent protein intensity profiles for the first frame of a migrating neuron sequence: (a,b) automated; (c,d) manual.

consistently higher than those in the manual profiles; we attribute this discrepancy to the fact that the contour evolution step in our approach (Sec. 2.2.2) adjusts the resulting trace to lie upon the highest intensity values along the cellular processes, whereas the manual traces are more prone to error and do not undergo any such adjustment.

4. CONCLUSIONS

The traces produced by the automated algorithm on our test dataset were typically within two pixels of those drawn by neurobiologists on the same images. We validated our results by quantitatively comparing traces from 50 frames taken from two different migrating neuron sequences. Because our algorithm attempts to maximize image brightness along the trace, the line intensity profiles generated along our automated traces tended to be slightly brighter than those generated from the manual traces. We observed that the most significant errors usually occurred near the tips of the leading and trailing processes, where the neuronal process tends to widen dramatically before coming to an end. This widening causes difficulty in defining a clear centerline. We also observed, in other video sequences, that somas or processes of other neurons intersecting the process of interest occasionally confused our algorithm; for this reason, the algorithm might be improved by simultaneous tracing of other neurons to resolve ambiguities arising from such intersections.

ACKNOWLEDGMENTS

Notice: This manuscript has been authored by UT-Battelle, LLC, under contract DE-AC05-00OR22725 with the U. S. Department of Energy. The United States Government retains and the publisher, by accepting the article for publication, acknowledges that the United States Government retains a non-exclusive, paid-up, irrevocable,

world-wide license to publish or reproduce the published form of this manuscript, or allow others to do so, for United States Government purposes. Research sponsored by the Laboratory Directed Research and Development Program of Oak Ridge National Laboratory (ORNL), managed by UT-Battelle, LLC for the U. S. Department of Energy.

REFERENCES

[1] Solecki, D. J., Trivedi, N., Govek, E.-E., Kerekes, R. A., Gleason, S. S., and Hatten, M. E., "Myosin II motors and f-actin dynamics drive the coordinated movement of the centrosome and soma during CNS glial-guided neuronal migration," *Neuron* **63**, 63–80 (2009).

[2] Losavio, B. E., Liang, Y., Santamaria-Pang, A., Kakadiaris, I. A., Colbert, C. M., and Saggau, P., "Live neuron morphology automatically reconstructed from multiphoton and confocal imaging data," *J. Neurophysiol.* **100**, 2422–2429 (2008).

[3] Al-Kofahi, K. A., Lasek, S., Swarowski, D. H., Pace, C. J., Nagy, G., Turner, J. N., and Roysam, B., "Rapid automated three-dimensional tracing of neurons from confocal image stacks," *IEEE Trans. Information Technology in Biomedicine* **6**, 171–187 (2002).

[4] Wearne, S., Rodriguez, A., Ehlenberger, D. B., Rocher, A. B., Henderson, S. C., and Hof, P. R., "New techniques for imaging, digitization, and analysis of three-dimensional neural morphology on multiple scales," *Neuroscience* **136**, 661–680 (2005).

[5] Xiong, G., Zhou, X., Degterev, A., Ji, L., and Wong, S. T. C., "Automated neurite labeling and analysis in fluorescence microscopy images," *Cytometry Part A* **69A**, 494–505 (2006).